



Estimation of bubble-mediated air–sea gas exchange from concurrent DMS and CO₂ transfer velocities at intermediate–high wind speeds

Thomas G. Bell¹, Sebastian Landwehr², Scott D. Miller³, Warren J. de Bruyn⁴, Adrian H. Callaghan^{5,a}, Brian Scanlon², Brian Ward², Mingxi Yang¹, and Eric S. Saltzman⁶

¹Plymouth Marine Laboratory, Prospect Place, The Hoe, Plymouth, PL1 3DH, UK

²School of Physics, National University of Ireland, Galway, Ireland

³Atmospheric Sciences Research Center, State University of New York at Albany, NY, USA

⁴Schmid College of Science and Technology, Chapman University, Orange, California, CA, USA

⁵Scripps Institution of Oceanography, University of California San Diego, 9500 Gilman Drive, La Jolla, CA 92093, USA

⁶Department of Earth System Science, University of California, Irvine, CA, USA

^anow at: Department of Civil and Environmental Engineering, Imperial College London, South Kensington Campus, London, SW7 2AZ, UK

Correspondence to: Thomas G. Bell (tbe@pml.ac.uk)

Received: 30 January 2017 – Discussion started: 9 February 2017

Revised: 7 June 2017 – Accepted: 28 June 2017 – Published: 27 July 2017

Abstract. Simultaneous air–sea fluxes and concentration differences of dimethylsulfide (DMS) and carbon dioxide (CO₂) were measured during a summertime North Atlantic cruise in 2011. This data set reveals significant differences between the gas transfer velocities of these two gases (Δk_w) over a range of wind speeds up to 21 m s⁻¹. These differences occur at and above the approximate wind speed threshold when waves begin breaking. Whitecap fraction (a proxy for bubbles) was also measured and has a positive relationship with Δk_w , consistent with enhanced bubble-mediated transfer of the less soluble CO₂ relative to that of the more soluble DMS. However, the correlation of Δk_w with whitecap fraction is no stronger than with wind speed. Models used to estimate bubble-mediated transfer from in situ whitecap fraction underpredict the observations, particularly at intermediate wind speeds. Examining the differences between gas transfer velocities of gases with different solubilities is a useful way to detect the impact of bubble-mediated exchange. More simultaneous gas transfer measurements of different solubility gases across a wide range of oceanic conditions are needed to understand the factors controlling the magnitude and scaling of bubble-mediated gas exchange.

1 Introduction

Air–sea exchange is a significant process for many compounds that have biogeochemical and climatic importance. Approximately 25 % of the carbon dioxide (CO₂) released into the atmosphere by anthropogenic activities has been taken up by the world oceans, which has tempered its climate forcing while leading to ocean acidification (Le Quéré et al., 2015). The biogenic gas dimethylsulfide (DMS) is a major contributor to the mass of marine atmospheric aerosol (Virkkula et al., 2006). Volatile organic compounds (VOCs) such as isoprene, acetone and acetaldehyde alter the oxidising capacity of the troposphere (Carpenter et al., 2012). The solubility differences between these VOCs mean that their exchange is controlled to differing degrees by processes on the water and air side of the air–sea interface (Yang et al., 2014). Many of the factors influencing air–sea gas exchange will be altered by future changes in climate, ocean circulation and biology. Earth system models and air quality models require more accurate understanding of the processes that influence air–sea gas transfer.

Air–sea gas exchange is typically parameterised as a function of the ocean–atmosphere bulk concentration difference (ΔC) and the physical mixing induced by wind stress at the

interface (Liss and Slater, 1974). The air–sea flux is typically described using the expression

$$\text{Flux} = K(C_w - \alpha C_a), \quad (1)$$

where C_w and C_a are the trace gas bulk concentration on either side of the interface, α is the dimensionless water/air solubility of the gas in seawater and K is the gas transfer velocity. The physics of gas transfer are implicitly represented by the gas transfer velocity, which is commonly expressed in water-side units of velocity (cm h^{-1}) and parameterised as a function of wind speed (U_{10}) and Schmidt number (Sc). The simplicity of Eq. (1) belies the complexity of the processes involved in air–sea gas transfer. These processes include diffusion, surface renewal and bubble-mediated transport. In turn, turbulence can be generated by wind stress, wave-induced mixing, buoyancy, currents and wave breaking. A variety of theoretical, laboratory and field approaches have been used to study the processes that control air–sea transfer, but we do not yet have a firm understanding of their relative importance under a range of atmospheric and oceanic conditions.

The gas-transfer–wind-speed relationships for gases of different solubility may be affected by breaking waves and bubbles (Keeling, 1993; Woolf, 1993, 1997). Gas invasion and evasion via bubbles (k_{bub}) is sensitive to the void fraction (ratio of air volume to total volume) of the bubble plume as well as the bubble size distribution. Bubble injection depth and cleanliness of the surface (influenced by surfactants) affect bubble rise velocity and residence time. Bubble residence time determines the time available for equilibration to occur while bubble volume, pressure and gas diffusivity (Sc) govern the time needed for a bubble to equilibrate. The magnitude of k_{bub} is expected to be greater for sparingly soluble gases (e.g. CO_2 , dimensionless solubility ~ 1) than for more soluble gases such as DMS (dimensionless solubility ~ 15), particularly when bubbles are fully equilibrated. Bubble-mediated gas transfer has been studied in the laboratory (Asher et al., 1996; Rhee et al., 2007) and using models (e.g. Woolf, 2005; Woolf et al., 2007; Fairall et al., 2011; Goddijn-Murphy et al., 2016).

Deliberate, dual-tracer techniques have estimated gas transfer by measuring the evasion of a pair of sparingly soluble gases with different diffusivity (^3He and SF_6 , dimensionless solubility ≤ 0.01). These studies observed a non-linear wind speed dependence of the gas transfer velocity, in qualitative agreement with earlier studies in wind–wave tanks (e.g. Wanninkhof et al., 1985; Liss and Merlivat, 1986; Watson et al., 1991). Direct, shipboard measurements of water-side gas transfer have also been made by eddy covariance (e.g. McGillis et al., 2001; Huebert et al., 2004; Marandino et al., 2007; Miller et al., 2010; Bell et al., 2013). These measurements typically show DMS gas transfer velocities that are lower and exhibit more linear wind speed dependence than the CO_2 transfer velocity–wind speed relationship inferred from dual-tracer studies (e.g. Yang et al., 2011;

Goddijn-Murphy et al., 2012; Bell et al., 2015). It has been suggested that the difference between the open-ocean gas transfer velocities of CO_2 and DMS is due to the reduced importance of bubble-mediated exchange for DMS (Blomquist et al., 2006; Fairall et al., 2011; Goddijn-Murphy et al., 2016).

Only one set of concurrent CO_2 and DMS gas transfer velocity measurements have been published to date (Miller et al., 2009). In that study, no data were collected for winds greater than 10 m s^{-1} and no statistically significant difference was observed in the CO_2 and DMS gas transfer–wind speed relationships after normalising both gases to a common diffusivity. This study presents a more extensive set of CO_2 and DMS gas transfer velocities that were measured simultaneously aboard the R/V *Knorr* in the 2011 summertime North Atlantic in both oligotrophic and highly productive waters. The DMS gas transfer velocities are discussed separately in detail by Bell et al. (2013). Here we focus specifically on what can be learned about gas transfer from the differences in behaviour of two different solubility gases at intermediate and high wind speeds.

2 Methods

2.1 Seawater, atmospheric and flux measurement systems

The measurement setups for DMS and CO_2 concentrations in air and water and the eddy covariance flux systems have been discussed in detail elsewhere (Miller et al., 2008; Saltzman et al., 2009; Miller et al., 2010; Bell et al., 2013, 2015; Landwehr et al., 2014; Landwehr et al., 2015). We provide a summary plus some additional details in the Appendix.

2.2 Gas transfer velocity calculations

In this section we describe the calculation of DMS and CO_2 gas transfer velocities from the Knorr_11 cruise data. Measured gas transfer velocities are transformed into water-side-only gas transfer velocities in order to remove the influence of air-side resistance. The relative contribution of air-side resistance to the total resistance is a function of solubility and thus different for the two gases. Finally, we discuss the most appropriate approach for comparing the water-side gas transfer velocities, given that the two gases have different molecular diffusivity and solubility.

Total gas transfer velocities (K) are calculated for CO_2 and DMS for each 10 min flux interval of the Knorr_11 cruise using Eq. (1). The temperature-dependent dimensionless solubilities of CO_2 and DMS in seawater are calculated following Weiss (1974) and Dacey et al. (1984) respectively. These gas transfer velocities reflect the result of resistance on both sides of the interface (Liss and Slater, 1974). The water-side

contribution to the total resistance is determined as follows:

$$k_w = \left[\frac{1}{K} - \frac{\alpha}{k_a} \right]^{-1}, \quad (2)$$

where k_w and k_a are the air-side and water-side gas transfer velocities and α is dimensionless water/air solubility. Note that we use the α reported by Dacey et al. (1984) in these calculations rather than the Henry law constant (H , units of atm L mol^{-1}) as there appears to be an error in conversion between α and H in that study (see Supplement discussion). CO_2 solubility is sufficiently low that air-side resistance is negligible and the water-side gas transfer is assumed equal to the total transfer velocity ($k_{\text{CO}_2} = K_{\text{CO}_2}$). The air-side resistance for DMS needs to be accounted for because it is a moderately soluble gas (McGillis et al., 2000). Air-side gas transfer velocities (k_a) for DMS were calculated for each 10 min flux interval with the NOAA COAREG 3.1 model, using sea surface temperature (SST) and horizontal wind speed measured during the cruise. The NOAA COAREG 3.1 model (Fairall et al., 2011) is an extension of the COARE bulk parameterisation for air–sea energy and momentum fluxes to parameterise gas transfer (Fairall et al., 1996, 2000). The air-side resistance contributes about 5% on average to the total resistance for DMS. NOAA COAREG 3.1 model calculations were carried out using a turbulent/molecular coefficient, $A = 1.6$, and bubble-mediated coefficient, $B = 1.8$ (Fairall et al., 2011). Knorr_11 measurements of SST, air temperature, relative humidity, air pressure, downward radiation and wind speed were used as input parameters to the model. Note that the use of the COAREG 3.1 model introduces a small uncertainty in our estimates of water-side DMS gas transfer velocity (approximately $\pm 2\%$ when wind speed = 20 m s^{-1}).

To facilitate comparison of transfer coefficients for the two gases across a range of sea surface temperatures, gas transfer velocities are corrected for changes in molecular diffusivity and viscosity. The correction typically involves the normalisation of water-side gas transfer velocities to a common Schmidt number ($Sc = 660$), equivalent to CO_2 in seawater at 20°C :

$$k_{X,660} = k_X \cdot \left(\frac{660}{Sc_X} \right)^{-0.5}, \quad (3)$$

where subscript X refers to CO_2 or DMS (i.e. $k_{\text{DMS},660}$ and $k_{\text{CO}_2,660}$). Temperature-dependent Sc_{CO_2} and Sc_{DMS} were obtained using the in situ seawater temperature from the ship's bow sensor and parameterisations from Wanninkhof (1992) and Saltzman et al. (1993).

The Sc number normalisation (Eq. 3) is commonly used across the whole range of wind speeds. In fact, it is only appropriate at low or moderate winds when interfacial gas transfer dominates over bubble-mediated gas exchange. If bubbles are an important component of gas transfer then solubility also plays a role and normalisation based on Sc alone may not be sufficient.

To develop a more rigorous comparison of k_{DMS} and k_{CO_2} , we normalised the water-side transfer velocities of DMS to the Schmidt number of CO_2 at the in situ sea surface temperature of each 10 min flux interval, as follows:

$$k_{\text{DMS},Sc} = k_{\text{DMS}} \cdot \left(\frac{Sc_{\text{CO}_2}}{Sc_{\text{DMS}}} \right)^{-0.5}, \quad (4)$$

where Sc_{CO_2} and Sc_{DMS} are the Schmidt numbers of CO_2 and DMS at the in situ sea surface temperature. Compared to normalising both DMS and CO_2 to $Sc = 660$, this approach has the advantage of correcting only k_{DMS} , with no correction to k_{CO_2} . The Sc correction for DMS should be reasonably accurate, assuming that the bubble-mediated transfer for the more soluble DMS is relatively small.

On the Knorr_11 cruise, the variability in sea surface temperature was small ($1\sigma = \pm 1^\circ\text{C}$). As a result, there is little difference in the variability or wind speed dependence of Sc -corrected k_{CO_2} compared to k_{CO_2} at the in situ temperature (Fig. 5 vs. Fig. S5 in Supplement). In Sect. 3.4, the relationship between CO_2 and DMS gas transfer velocities and wind speed is examined using $k_{\text{DMS},Sc}$ and k_{CO_2} .

2.3 Calculation of $k_{\text{bub},\text{CO}_2}$

The flux of a water-side controlled gas is equal to the sum of the interfacial flux and the bubble-mediated flux. For gases with significant air–sea disequilibrium these processes are often considered as parallel transfer velocities, i.e. total transfer velocity $k_w = k_{\text{int}} + k_{\text{bub}}$. See Woolf (1997) for a more complete discussion of bubble-mediated transfer for gases close to ocean–atmosphere equilibrium. We assume that turbulence and diffusive mixing at the sea surface operate similarly upon the interfacial air–sea transfer of CO_2 and DMS (i.e. $k_{\text{int},\text{CO}_2} = k_{\text{int},\text{DMS}}$), given appropriate normalisation for the differences in molecular diffusivity. Observed differences between $k_{\text{DMS},Sc}$ and k_{CO_2} should therefore be a measure of the difference between the bubble-mediated contributions to DMS and CO_2 gas transfer:

$$\Delta k_w = k_{\text{bub},\text{CO}_2} - k_{\text{bub},\text{DMS}}. \quad (5)$$

Strictly speaking, Eq. (5) should also account for the influence of bubble overpressure, which alters the gas flux due to bubbles when the concentration gradient is into the ocean. The extra pressure on the gas in the bubbles is calculated following Woolf (1997): $\Delta = (U_{10}/U_i)^2 \%$ where U_i is the wind speed at which the supersaturation of a particular gas equals 1% (49 m s^{-1} in the case of CO_2). A high wind speed (20 m s^{-1}) gives $\Delta = 0.167\%$, which would lead to only a $\sim 2\%$ enhancement of the CO_2 flux when the air–sea concentration gradient is 30 ppm (minimum for this study) and into the ocean. The magnitude of this effect would be larger for gases less soluble than CO_2 but we are able to ignore it for the purposes of this study.

$k_{\text{bub},\text{CO}_2}$ and $k_{\text{bub},\text{DMS}}$ are related by the influence of solubility and diffusivity upon bubble-mediated transfer. We pa-

parameterise this relationship simply as $k_{\text{bub,DMS}} = f k_{\text{bub,CO}_2}$. Substitution into Eq. (5) yields

$$k_{\text{bub,CO}_2} = \frac{\Delta k_w}{1 - f}. \quad (6)$$

The value of f depends on seawater temperature and the complex dynamics of bubble formation and cycling (size distributions, surfactants, etc.). At the mean SST encountered in this study (9.8 °C), the bubble gas transfer models of Woolf (1997) and Asher (Asher and Wanninkhof, 1998; Asher et al., 2002) yield values for f of 0.14 and 0.28, respectively (see Supplement for model equations).

2.4 Sea surface imaging

Whitecap areal fraction was measured using images of the sea surface recorded with a digital camera (5-megapixel Arecont Vision, 16 mm focal length lens) mounted 14.6 m above the ocean surface at an angle of $\sim 75^\circ$ from the nadir. Image footprints represent $\sim 7600 \text{ m}^2$ of sea surface. Images were collected at a sample interval of about 1 s and post-processed for whitecap fraction according to the automated whitecap extraction algorithm method (Callaghan and White, 2009). More detail on the methodology, camera exposure settings and data comparability are provided in the Supplement. Images were further processed to distinguish whitecap pixels as either stage A or stage B whitecaps by applying a spatial separation technique (Scanlon and Ward, 2013). The whitecap fraction measurements were averaged in the same way as the gas transfer velocities (i.e. time-averaged mean values as well as 2 m s^{-1} wind speed bins).

3 Results

3.1 Cruise location and environmental conditions

This study took place in the summertime North Atlantic (24 June–18 July 2011; DOY 175–199), departing and returning to Woods Hole, MA. Most of the data were collected north of 50° N , including the occupation of four 24–36 h stations – ST181, ST184, ST187 and ST191 (Fig. 1). The cruise track was designed to sample regions with high biological productivity and phytoplankton blooms, with large air–sea concentration differences for CO_2 and DMS. The cruise meteorology and physical oceanography is discussed in detail by Bell et al. (2013). A series of weather systems travelling from West to East passed over the region during the cruise. Wind speeds ranged from ~ 1 to 22 m s^{-1} , with strongest winds during the frontal passages at stations ST184 and ST191 (Fig. 1b). Atmospheric boundary layer stability was close to neutral for most of the cruise ($|z/L| < 0.07$; 75 % of the time), with infrequent stable conditions ($z/L > 0.05$; < 8 % of the time, Fig. 1a). There was no evidence that the stable periods affected the flux measurements (Bell et al., 2013). White-

cap areal fraction increased up to a maximum of ~ 0.06 in response to high wind speeds (Fig. 1b).

3.2 Whitecaps

Whitecaps were observed during Knorr_11 when wind speeds exceeded 4.5 m s^{-1} , a typical wind speed threshold for whitecap formation in the open ocean (Callaghan et al., 2008; Schwendeman and Thomson, 2015). Whitecap areal fraction is a strong, non-linear function of wind speed (Fig. 2a). The whitecap vs. wind speed relationship for Knorr_11 is similar in shape to recently published wind-speed-based whitecap parameterisations (Callaghan et al., 2008; Schwendeman and Thomson, 2015). At intermediate wind speeds the Knorr_11 whitecap data are lower than the parameterisations (Fig. 2a). Total whitecap coverage is a function of (i) active “stage A whitecaps” (W_A) produced from recent wave breaking and (ii) maturing “stage B whitecaps” (W_B) that are decaying foam from previous breakers. The Stage A whitecap fraction data are highly variable at $\sim 11 \text{ m s}^{-1}$ wind speeds (Fig. 2b), which is driven by the difference in the wind–wave conditions during Knorr_11 (see discussion in Supplement).

3.3 Concentrations, fluxes and gas transfer velocities

Seawater $p\text{CO}_2$ was consistently lower than the overlying atmosphere throughout the study region due to biological uptake (Fig. 3a). As a result, the air–sea concentration difference ($\Delta p\text{CO}_2$) was large and always into the ocean, with $\Delta p\text{CO}_2 < -45 \text{ ppm}$ for more than 80 % of the measurements. Periods with particularly enhanced $\Delta p\text{CO}_2$ into the ocean were during the transit between ST181 and ST184 ($\Delta p\text{CO}_2$ as large as -120 ppm) and during ST191 ($\Delta p\text{CO}_2$ consistently -75 ppm).

Seawater DMS levels were much higher than atmospheric levels, reflecting the biogenic sources in seawater and the relatively short atmospheric lifetime (~ 1 day; Kloster et al., 2006). The largest air–sea DMS concentration differences (ΔDMS) of 6–12 ppb were observed during DOY 185–190 (Fig. 4a). The ΔDMS and $\Delta p\text{CO}_2$ did not co-vary (Spearman $\rho = 0.11$, $n = 918$, $p < 0.001$). This is not surprising because, although seawater DMS and CO_2 signals are both influenced by biological activity, they are controlled by different processes. Seawater CO_2 levels reflect the net result of community photosynthesis and respiration, while DMS production is related to metabolic processes that are highly species-dependent (Stefels et al., 2007).

CO_2 fluxes (F_{CO_2}) were generally into the ocean, as expected given the direction of the air–sea concentration difference (Fig. 3b). The variability in F_{CO_2} observed on this cruise reflects dependence on both wind speed and $\Delta p\text{CO}_2$. For example, during DOY182 air-to-sea CO_2 fluxes increase due to a gradual increase in $\Delta p\text{CO}_2$ with fairly constant wind speed. More commonly, $\Delta p\text{CO}_2$ was fairly constant and

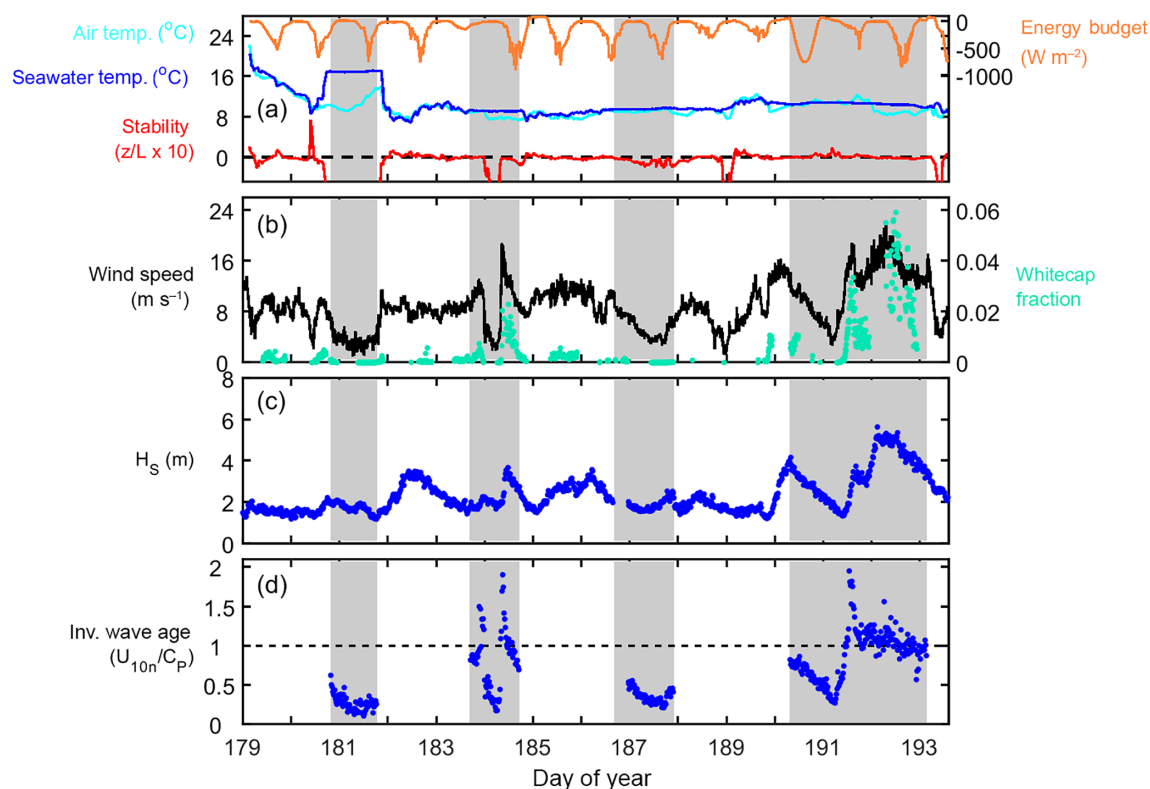


Figure 1. Time series of 10 min averaged data collected during the Knorr_11 cruise. Dashed black line in panel (a) indicates neutral atmospheric stability ($z/L = 0$). Grey shaded regions represent intervals when the ship occupied stations ST181, ST184, ST187, and ST191. Measured wave properties (see Bell et al., 2013) are presented in panels (c) and (d): significant wave height H_s (c) and inverse wave age (d). $U_{10n}/C_p \geq 1$ represent younger seas and $U_{10n}/C_p < 1$ represent older seas.

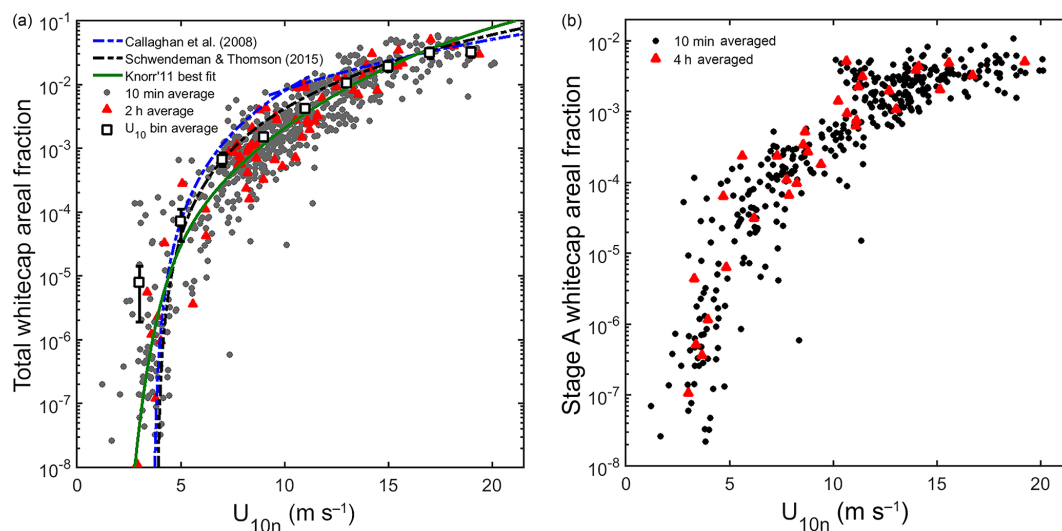


Figure 2. Semi-log plots of whitecap areal fraction as a function of mean horizontal wind speed at 10 m above the sea surface (U_{10n}) during the Knorr_11 cruise. 10 min average (grey dots) and 2 h average (red triangles) data are shown on both panels. (a) Total whitecap area (W_T) versus U_{10n} bin-averaged data (open squares, 2 m s^{-1} bins). The best fit line to Knorr_11 2 h average data (green; $\log_{10}(W_T) = -42.19e^{(-0.95U)} - 6.5e^{(-0.0886U)}$) and wind speed parameterisations from the recent literature are shown for reference. (b) Whitecap area considered to be solely from wave breaking (Stage A whitecaps (W_A); see text for definition).

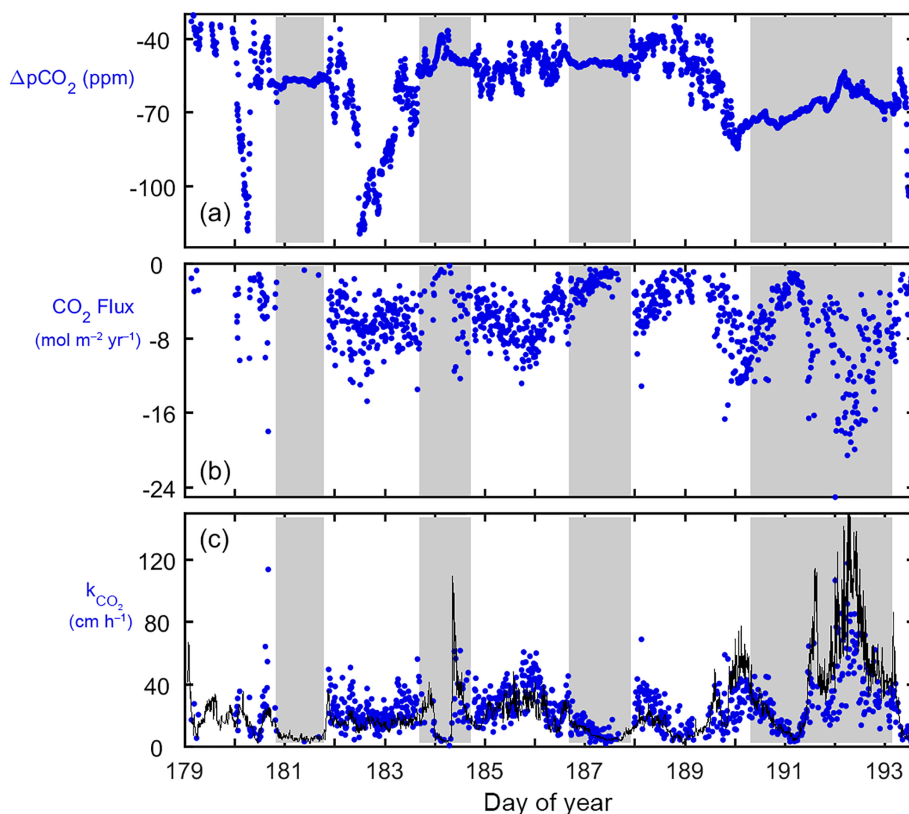


Figure 3. Knorr_11 cruise time series of 10 min averaged CO₂: (a) air–sea concentration difference ($\Delta p\text{CO}_2$), (b) flux (F_{CO_2}) and (c) gas transfer velocity (k_{CO_2} ; water side only, no Sc correction). Panel (c) also shows k_{CO_2} calculated using the NOAA COARE model (black line). Note that negative k_{CO_2} data points in (c) were omitted for clarity (see Fig. S6 for full data set). Grey shaded regions represent periods on station.

variability in F_{CO_2} reflected changes in wind speed. For example, from DOY 185 to 187 wind speeds gradually declined from ~ 10 to 5 m s^{-1} with a concurrent decline in F_{CO_2} . DMS eddy covariance fluxes were always out of the ocean. The 10 min averaged DMS fluxes (F_{DMS}) clearly show the influence of ΔDMS (e.g. DOY 188) and wind speed (e.g. DOY 184).

Gas transfer velocities of CO₂ and DMS from this cruise exhibit two systematic differences: (i) k_{DMS} values are generally lower than k_{CO_2} , particularly during episodes of high wind speed; and (ii) k_{CO_2} is characterised by much larger scatter than k_{DMS} . We attribute the large scatter in k_{CO_2} to the greater random uncertainty associated with the eddy covariance measurement of air–sea CO₂ fluxes compared to those of DMS. As shown by Miller et al. (2010), the analytical approach used in this study (dried air, closed path LI7500) has sufficient precision to adequately resolve the turbulent fluctuations in atmospheric CO₂ associated with the surface flux over most of the cruise ($\Delta p\text{CO}_2 < -30$ ppm). The scatter in the CO₂ flux measurements is more likely due to environmental variability resulting from fluctuations in boundary layer CO₂ mixing ratio arising from horizontal and/or vertical transport unrelated to air–sea flux (Edson et al., 2008;

Blomquist et al., 2014). These effects likely have a much smaller effect on air–sea DMS fluxes, because the air–sea DMS concentration difference is always much larger than the mean atmospheric DMS concentration (due to the short atmospheric lifetime of DMS). For example, a $\Delta p\text{CO}_2$ of 100 ppm at a wind speed of 10 m s^{-1} will produce turbulent fluctuations that are $\sim 0.02\%$ of the background CO₂ on average. In contrast, a typical seawater DMS concentration (2.6 nM) at a wind speed of 6 m s^{-1} generates fluctuations that are 20 % of the background (Table 1; Blomquist et al., 2012). Thus, F_{CO_2} measurements are highly sensitive to small fluctuations in background CO₂ and the relative uncertainty is expected to be much larger than that for F_{DMS} .

3.4 Comparison of k_{CO_2} and $k_{\text{DMS},Sc}$

The differences between CO₂ and DMS gas transfer velocities observed in the time series are also evident when the data are examined as a function of wind speed. From the 10 min averaged data, it is clear that k_{CO_2} is greater than k_{DMS} and has a stronger wind speed dependence over most of the wind speed range (Fig. 5a, b). These broad trends are also easily seen in longer time-averaged data. Flux and ΔC measure-

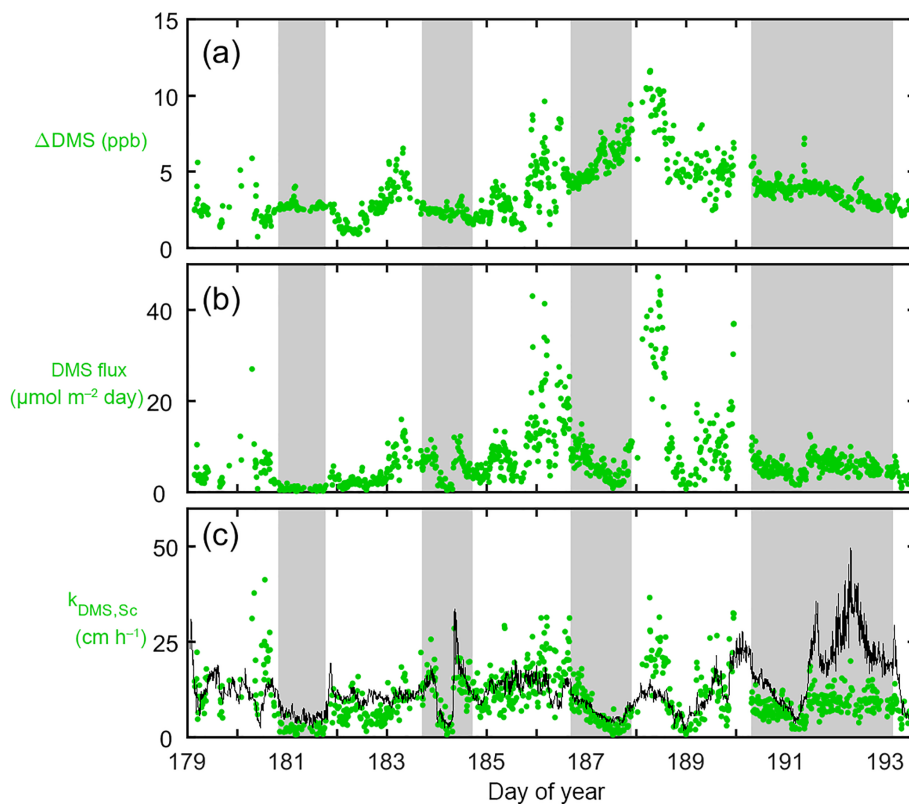


Figure 4. Knorr_11 cruise time series of 10 min averaged DMS: (a) air–sea concentration difference (ΔDMS), (b) flux (F_{DMS}) and (c) gas transfer velocity normalised to the in situ CO_2 Sc number ($k_{\text{DMS},Sc}$). Panel (c) also shows $k_{\text{DMS},Sc}$ calculated using NOAA COARE model output (black line). Grey shaded regions represent periods on station.

ments were averaged into 2 h periods (minimum of three flux intervals per 2 h period), which reduced the scatter in F_{CO_2} while preserving the temporal variability (see Fig. S7). Gas transfer velocities were then recalculated from the 2 h averaged data. 10 min k_{CO_2} and $k_{\text{DMS},Sc}$ data were also averaged into 2 m s^{-1} wind speed bins, with a minimum of five 10 min periods per bin. The 2 h averaged data and the wind speed binned data show k_{CO_2} and $k_{\text{DMS},Sc}$ diverging at intermediate wind speeds, differing by a factor of roughly 2 at 10 m s^{-1} (Fig. 5c, d).

DMS gas transfer velocities on this cruise exhibit complex behaviour at intermediate to high wind speeds, as discussed in Bell et al. (2013). $k_{\text{DMS},Sc}$ increases linearly with wind speed up to $\sim 11 \text{ m s}^{-1}$ (Fig. 5). Under the sustained high-wind, high-wave conditions encountered during ST191, the wind speed dependence of $k_{\text{DMS},Sc}$ was lower than expected, with a slope roughly half that of the rest of the cruise data. This effect was not observed at ST184 – for detailed discussion, see Bell et al. (2013). Such coherent spatial-temporal variation means that wind speed bin averaging of the higher wind speed $k_{\text{DMS},Sc}$ may mask real variability in the relationship with wind speed. Relationships developed from wind speed bin-averaged gas transfer data should be interpreted

with caution, especially when it comes to developing generalisable air–sea gas transfer models.

The Knorr_11 k_{CO_2} data also demonstrate a clear wind speed dependence (Fig. 5). The NOAA COARE model for CO_2 has been tuned to previous eddy covariance flux measurements (McGillis et al., 2001), with bubble-mediated transfer determining the non-linear relationship with wind speed (Fairall et al., 2011). There is reasonable agreement between the COARE model gas transfer velocity predictions and the Knorr_11 k_{CO_2} data up to $\sim 11 \text{ m s}^{-1}$ wind speed. Above 11 m s^{-1} , the COARE model overpredicts k_{CO_2} . This could be interpreted as indicating high wind speed suppression of gas transfer for CO_2 as observed for DMS (as discussed by Bell et al., 2013). However, it is important to note that the number of high wind speed ($> 15 \text{ m s}^{-1}$) gas transfer measurements in this study is limited to 9 and 16 h of data for DMS and CO_2 respectively. Much more data are needed in order to firmly establish the high wind speed behaviour.

The COAREG 3.1 model parameterises interfacial gas transfer by scaling to Sc and friction velocity and estimates bubble-mediated gas transfer following Woolf (1997). The lower solubility of CO_2 leads to enhanced gas transfer relative to that of DMS at high wind speeds where bubble transport is significant (Fairall et al., 2011). There is good

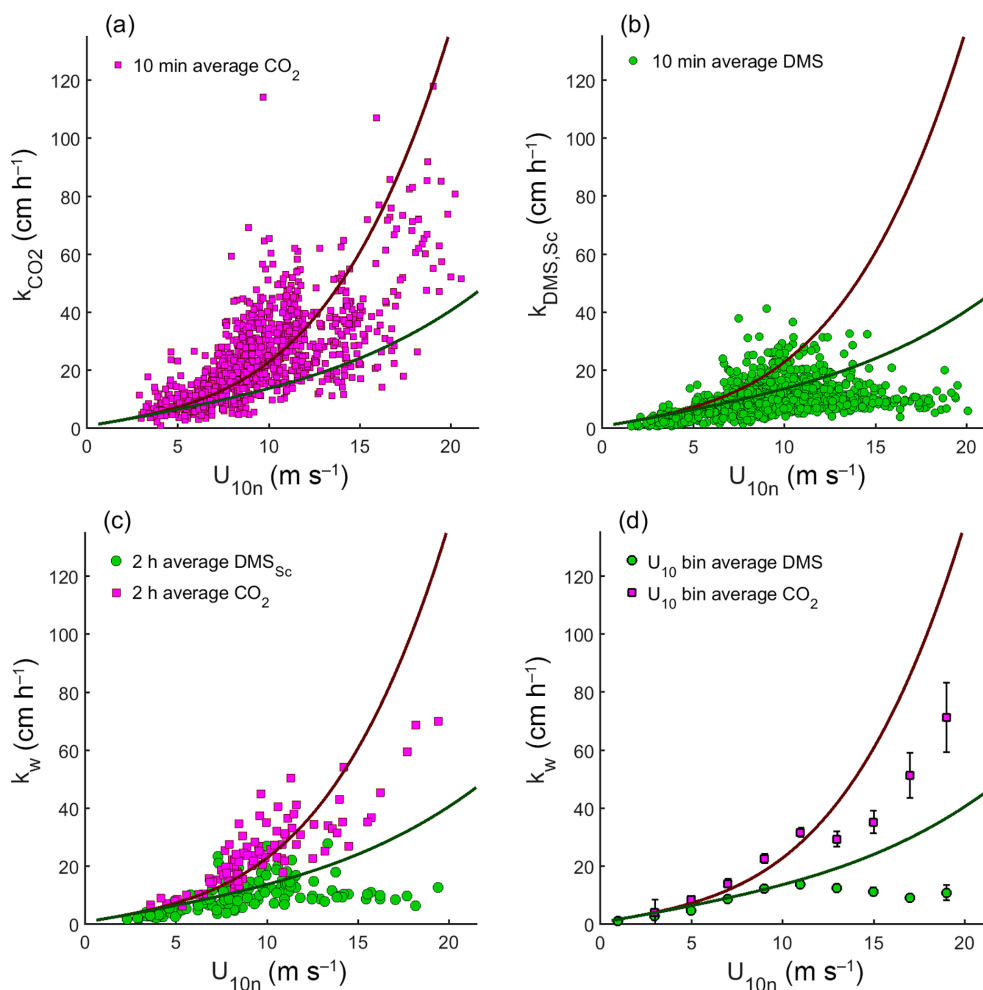


Figure 5. Gas transfer velocities plotted against mean horizontal wind speed (U_{10}) from the Knorr_11 cruise: 10 min average data for CO_2 (a) and DMS (b). DMS gas transfer velocities are normalised to the in situ CO_2 Sc number. Data are averaged into 2 h periods (c) and 2 m s^{-1} wind speed bins (d). Note that negative k_{CO_2} data in (a) have not been plotted for clarity (see Fig. S8 for full data set). For reference, the NOAA COAREG3.1 model output for CO_2 (magenta line) and DMS (green line) is plotted on all four panels. The COARE model was run with the turbulent/molecular coefficient, $A = 1.6$, and the bubble-mediated coefficient, $B = 1.8$, and used mean Knorr_11 data for the input parameters.

agreement between the COAREG model gas transfer velocity predictions and the Knorr_11 k_{CO_2} and k_{DMS} data until $\sim 11 \text{ m s}^{-1}$ wind speed.

Earlier in this paper we introduced the quantity Δk_w as an observational measure of the difference in gas transfer velocities of CO_2 and DMS (Sect. 2.3, Eq. 6). The relationship between Δk_w and wind speed is positive and shows no systematic differences related to temporal variability (Fig. 6). Sea surface temperature (SST) is indicated by symbol size. Some of the scatter in Fig. 6 could be driven by changes in Sc due to SST variability. Nearly all of the data in Fig. 6 are from periods when SST was relatively constant ($9.7 \pm 1.1^\circ \text{C}$). Many of the k_{CO_2} data with warm seawater (i.e. ST181, $\text{SST} > 12^\circ \text{C}$) were rejected by our quality control criteria (see Appendix A3). These data were collected when wind

speeds were low, which resulted in small CO_2 fluxes with large variability at low frequencies. Of the periods with $\text{SST} > 12^\circ \text{C}$ that passed the quality control criteria, the majority contributed fewer data within a 2 h averaging period than the minimum threshold (three 10 min averaged data points).

4 Discussion

The bubble-mediated component of gas transfer is a strong function of wind speed and breaking waves. Previous estimates of bubble-mediated air–sea gas exchange have used data from laboratory experiments (Keeling, 1993; Asher et al., 1996; Woolf, 1997). The differences between gas transfer velocities for DMS and CO_2 provide a unique way to constrain the importance of bubble-mediated transfer under

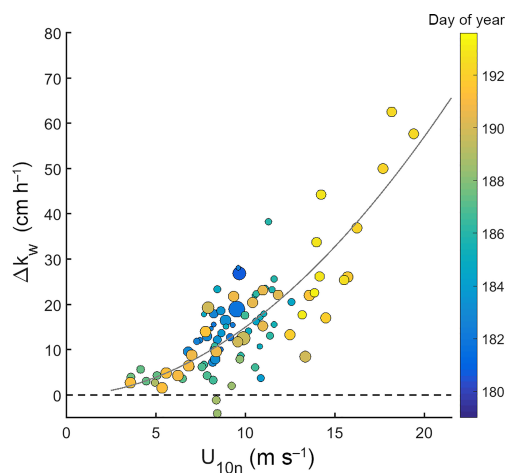


Figure 6. Difference (Δk_w) between 2 h average k_{CO_2} and $k_{\text{DMS},Sc}$ plotted against U_{10} . Data are coloured by the date of measurement (Day of Year). Sea surface temperature (SST) is indicated by symbol size (range is 7.1 to 12.5 °C). The solid grey line describes the power law fit to the data (see Eq. 7).

natural conditions. This study shows that Δk_w is near zero ($< 4.5 \text{ cm h}^{-1}$) at low wind speeds ($U_{10} \leq 4.5 \text{ m s}^{-1}$), which is consistent with the wind speed at which whitecap fraction becomes significant ($W_T > 10^{-5}$, Fig. 2a). Above 4.5 m s^{-1} , Δk_w increases non-linearly, consistent with an increase in bubble-mediated CO_2 transfer associated with wave breaking. The relationship between Δk_w and wind speed is non-linear, and a power law wind speed dependence yields a good fit ($R^2 = 0.66$; Fig. 6):

$$\Delta k_w = 0.177 U_{10}^{1.928}. \quad (7)$$

The functional form of this relationship is qualitatively consistent with those found between U_{10} and breaking waves/wave energy dissipation (Melville and Matusov, 2002) and U_{10} vs. whitecap areal fraction (e.g. Callaghan et al., 2008; Schwendeman and Thomson, 2015). Bubble-mediated gas transfer is the only viable explanation for the magnitude and wind speed dependence of Δk_w . The only alternative explanation would require a large systematic bias in the measurement of relative gas transfer velocities of DMS and CO_2 . There are no obvious candidates for such biases.

During strong wind/large wave conditions, the Knorr_11 data suggest that bubble-mediated exchange is a dominant contributor to the total transfer of CO_2 . For example, when wind speeds were 11–12 m s^{-1} , Δk_w was about 50 % of the total CO_2 gas transfer (k_{CO_2}). A significant contribution by bubbles to the total gas transfer velocity means that bubble-mediated exchange must be included and adequately parameterised by gas transfer models. The Schmidt number (Sc) normalisation (Eq. 4) assumes that the gas transfer velocity is purely interfacial. An alternative normalisation (involving Sc and solubility) is required when bubble-mediated transfer is significant. Our data suggest that the current Sc normalisation

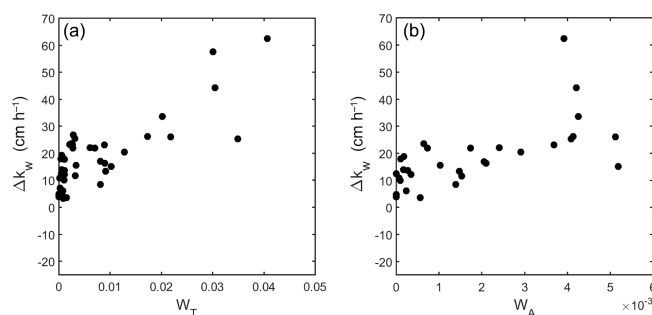


Figure 7. Knorr_11 Δk_w data plotted against total whitecap areal fraction (a) and against Stage A whitecap areal fraction (b). Each point is a 2 h average of coincident measurements of whitecap fraction and DMS and CO_2 gas transfer.

should be applied with caution to gas transfer data for different solubility gases at wind speeds greater than 10 m s^{-1} .

If Δk_w reflects the difference between the bubble-mediated contribution to the transfer of CO_2 and DMS, one would expect Δk_w to correlate with wave-breaking, and hence with the areal coverage of whitecaps. Breaking waves generate plumes of bubbles (Stage A whitecaps, W_A), which then rise to the surface and persist for a short period as foam (Stage B whitecaps, W_B). Almost all whitecap measurements represent the fraction of the sea surface that is covered by bubble plumes and/or foam – i.e. $W_T = W_A + W_B$. The Δk_w is positively correlated with both W_T (Spearman $\rho = 0.65$, $n = 43$, $p < 0.001$) and W_A (Spearman $\rho = 0.74$, $n = 32$, $p < 0.001$; Fig. 7a, b). These correlations are approximately the same strength as the correlation between Δk_w and wind speed (Spearman $\rho = 0.73$, $n = 88$, $p < 0.001$). The functional form of the relationship between Δk_w and whitecap areal extent appears to be linear for $W_T > 0.005$. However, the Knorr_11 data set is small and quite scattered, particularly when $W_T < 0.005$. More data are required to fully test the validity of whitecap areal fraction as a proxy for bubbles and bubble-mediated exchange.

Observations of the decaying white cap signal (W_B) suggest that the persistence of surface foam is related to both bubble plume depth (deeper bubble plumes take longer to degas) and sea surface chemistry (Callaghan et al., 2013). As measured here, W_B is approximately an order of magnitude larger than W_A and thus dominates the W_T signal. It is often assumed that gas exchange takes place in bubble plumes formed by active wave breaking (i.e. W_A), while W_B may vary widely due to surfactant concentration with little or no impact upon bubble-mediated gas exchange (e.g. Pereira et al., 2016). In this case, Δk_w should be more strongly correlated with W_A than W_B or W_T . The Knorr_11 data do not suggest that W_A is an improvement upon either W_T or even wind speed as a measure of bubble-mediated exchange. This may be because whitecaps do not fully represent the bubbles facilitating gas exchange as these may dissolve before

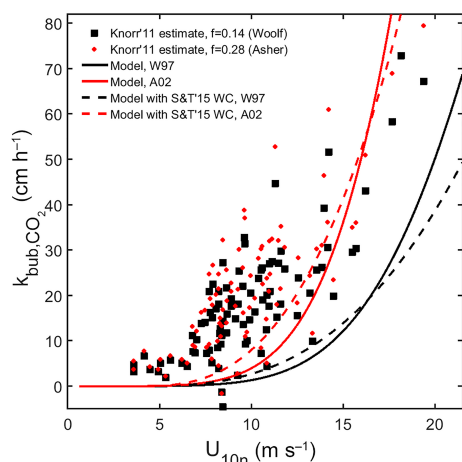


Figure 8. Bubble-mediated transfer velocity of CO_2 ($k_{\text{bub},\text{CO}_2}$) as a function of wind speed. Individual points are Knorr_11 observations using solubility and diffusivity scaling from Woolf (1997) (black squares) and Asher et al. (2002) (red circles). Continuous lines are model calculations of $k_{\text{bub},\text{CO}_2}$ using the Knorr_11 wind speed versus whitecap areal fraction relationship (see Fig. 2) and mean SST (Woolf, 1997: black; Asher et al., 2002: red). Model calculations were also performed using the Schwendeman and Thomson (2015) wind speed versus whitecap areal fraction relationship (dashed lines).

they reach the sea surface. Alternatively, W_T and W_A may be equally good (or poor) proxies for bubbles because: (i) surfactant activity was either insignificant or sufficiently invariant in the study region (despite high biological productivity) that W_B does not confound the relationship between W_T and W_A ; (ii) W_A is no better than W_T at representing the volume of air entrained by breaking waves; and/or (iii) bubbles residing at the surface (i.e. W_B) continue to contribute to gas transfer (Goddijn-Murphy et al., 2016).

As shown earlier, the bubble-mediated contribution to gas transfer ($k_{\text{bub},\text{CO}_2}$) can be obtained from Δk_w using information from mechanistic bubble gas transfer models (f ; see Sect. 2.3). The $k_{\text{bub},\text{CO}_2}$ data sets derived from the Knorr_11 data using the Asher (Asher and Wanninkhof, 1998; Asher et al., 2002) and Woolf (1997) models differ by about 15 % (Fig. 8). The field-based estimates of $k_{\text{bub},\text{CO}_2}$ can also be compared to model-only estimates for the Knorr_11 conditions using the Asher and Woolf models. Both models are based on total whitecap areal fraction, W_T . A non-linear fit of the Knorr_11 W_T and wind speed measurements ($W_T = 1.9 \times 10^{-6} U_{10m}^{3.36}$) was used to drive both models (Fig. 8). The Asher et al. (2002) model is based on laboratory tipping bucket gas evasion experiments (Asher et al., 1996) and the model was then adjusted to represent the flux of CO_2 into the ocean (invasion). Woolf (1997) scaled a single bubble model to the open ocean based on laboratory experiments.

Both models significantly underestimate $k_{\text{bub},\text{CO}_2}$ at wind speeds below about 11 m s^{-1} . At higher wind speeds, the Asher et al. (2002) model increases rapidly with wind speed to agree better with the Knorr_11 data. In contrast, Woolf (1997) consistently underestimates $k_{\text{bub},\text{CO}_2}$ at all wind speeds. Both $k_{\text{bub},\text{CO}_2}$ models depend on the choice of wind speed versus whitecap parameterisation. Using the Schwendeman and Thomson (2015) whitecap parameterisation instead of the Knorr_11 best fit makes some difference to the model output, but not enough to adequately fit to the data (Fig. 8). A “dense plume model” was also developed by Woolf et al. (2007) to take account of the interaction of a bubble plume with the interstitial water between bubbles. This model yields estimates of $k_{\text{bub},\text{CO}_2}$ that are even lower than the original Woolf (1997) “single bubble model” (data not shown).

It is likely that the Knorr_11 cruise data will be compared with estimates of $k_{\text{bub},\text{CO}_2}$ derived from future field campaigns, which will be conducted under different environmental conditions. Our $k_{\text{bub},\text{CO}_2}$ data are at in situ seawater temperature ($\sim 10^\circ\text{C}$) and thus in situ CO_2 solubility ($\alpha = 1.03$) and diffusivity ($Sc = 1150$). We use the Asher et al. (2002) and Woolf (1997) bubble models to make estimates of $k_{\text{bub},\text{CO}_2}$ normalised to a standard seawater temperature of 20°C ($k_{\text{bub},\text{CO}_2,20^\circ\text{C}}$, where $\alpha = 0.78$ and $Sc = 666$). The 2 h averaged Knorr_11 cruise data, including estimates of Δk_w , $k_{\text{bub},\text{CO}_2}$ and $k_{\text{bub},\text{CO}_2,20^\circ\text{C}}$, are provided in Supplemental Table S1.

The approach used in this study to estimate Δk_w and $k_{\text{bub},\text{CO}_2}$ from the Knorr_11 field data neglects the effect of sea surface skin temperature and CO_2 chemical enhancement. Skin temperature is typically only a few tenths of a degree less than bulk seawater under the conditions encountered in this study (Fairall et al., 1996). The impact upon k_{CO_2} due to skin temperature effects on CO_2 solubility and carbonate speciation is probably of the order of 3 % (Woolf et al., 2016). There is a chemical enhancement of the CO_2 flux due to ionisation at the sea surface (Hoover and Berkshire, 1969). The effect on k_{CO_2} has been estimated to be up to about 8 % at a wind speed of $4\text{--}6 \text{ m s}^{-1}$ (Wanninkhof and Knox, 1996), which amounts to a maximum impact of a few cm h^{-1} . By neglecting these effects we have slightly overestimated Δk_w and $k_{\text{bub},\text{CO}_2}$, but the magnitude of these corrections would be small relative to the environmental scatter or measurement uncertainty.

5 Conclusions

The Knorr_11 concurrent measurements of DMS and CO_2 gas transfer velocities show significant differences in gas transfer between the two gases at intermediate–high wind speeds. These data indicate that (i) bubble-mediated gas transfer becomes significant for CO_2 at or above the threshold for wave-breaking and (ii) the wind speed dependence is

non-linear, with a similar functional form to proposed relationships predicting whitecap areal extent from wind speed. However, existing models of bubble-mediated gas transfer using the Knorr_11 in situ observations of whitecap fraction significantly underestimate the importance of this process.

There are a number of assumptions behind model estimates of bubble-mediated gas exchange (Goddijn-Murphy et al., 2016). Model bias can be crudely split into (i) uncertainties in the scaling of whitecap fraction to the bubble population (e.g. using Cipriano and Blanchard, 1981) and (ii) the relationship between gas exchange and bubble properties, which are predicted as a function of air entrainment into the surface ocean by a breaking wave, bubble injection depth, size distribution and mobility through the water (a function of surface cleanliness and surfactants). The underestimation of bubble-mediated CO₂ gas transfer by both models is particularly apparent at low–intermediate wind speeds and low whitecap fraction. This could indicate either that bubble production during microscale breaking is an important process for gas transfer or that the relationship between whitecap fraction and bubble population is poorly constrained.

In summary, the approach of using simultaneous measurements of multiple gases with different solubility appears to be a viable way to constrain the magnitude of bubble-mediated gas transfer. Analysis of additional sparingly soluble gases, such as methane or oxygenated hydrocarbons, would further strengthen this approach. A much larger data set, under a wider range of oceanographic conditions, is certainly needed. In particular, it would be useful to examine DMS and CO₂ gas transfer velocities in ocean regions with different temperatures, where the solubility of each gas is significantly different from this study.

Data availability. Relevant data for this paper can be found in Table S1 of the Supplement.

Appendix A

A1 Seawater CO₂ and DMS measurements

Seawater CO₂ and DMS were monitored in the supply of seawater pumped continuously through the ship from an intake on the bow located 6 m below the sea surface. CO₂ was equilibrated with air in a recirculating showerhead type system. Alternate air- and water-side *p*CO₂ were each measured for 5 min by the same infrared gas analyser (IRGA). Seawater DMS was equilibrated with DMS-free air in a tubular porous membrane equilibrator, operated in a single-pass, counterflow mode. DMS was measured at 1 Hz using chemical ionisation mass spectrometry and bin-averaged at 1 min intervals (UCI miniCIMS; Saltzman et al., 2009). DMS was calibrated by continuously pumping an internal standard of tri-deuterated, DMS (d₃-DMS) into the seawater flow just before the equilibrator. Details of the methods and instrumentation used for equilibration and detection of seawater DMS are described in Saltzman et al. (2009).

A2 Mast-mounted instrumentation and data acquisition

The eddy covariance system was mounted 13.6 m above the sea surface on the bow mast. Platform angular rates and accelerations were measured by two Systron Donner Motion Pak II (MPII) units. Three-dimensional winds and sonic temperature were measured by two Campbell CSAT3 sonic anemometers. Air sampling inlets for DMS and CO₂ were located at the same height as the anemometers and within 20 cm of the measurement region. GPS and digital compass output were digitally logged at 1 Hz. Winds were corrected for ship motion and orientation as described in Miller et al. (2008) and Landwehr et al. (2015). The eddy covariance data streams were logged in both analogue and digital format as described in Bell et al. (2013).

A3 High-frequency atmospheric DMS and CO₂ measurements

Atmospheric DMS measurements were made at 10 Hz using an atmospheric pressure chemical ionisation mass spectrometer located in a lab van (UCI mesoCIMS; Bell et al., 2013). Air was drawn to the instrument through a 28 m long 1/2 in OD Teflon tube. A subsample of the air stream was passed through a Nafion drier prior to entering the mass spectrometer. The measurement was calibrated using an internal gas standard of tri-deuterated DMS added to the inlet (see Bell et al., 2013).

Atmospheric CO₂ measurements were made on air drawn at 8 L min⁻¹ through a filtered inlet (90 mm diameter with 1 micron pore size, Savillex) near the sonic anemometers on the bow mast, through 5 m of 5.9 mm ID polyethylene-lined Dekabon tubing to two fast-response CO₂/H₂O IRGAs in an enclosure on the bow mast. The IRGAs were open-path-style sensors (LI7500, Licor Inc.) converted to a closed-path configuration (see Miller et al., 2010) and were plumbed in series. A Nafion multi-tube membrane drier (PD-200T, PermaPure) with 6 L min⁻¹ dry air counter flow was installed between the two IRGAs such that the upstream IRGA sampled undried air and the downstream IRGA sampled the same air after drying. This technique removes 97 % of the Webb Correction from the measured CO₂ flux (first shown by Miller et al., 2010, and confirmed by Landwehr et al., 2014).

The air flow through both the CO₂ and DMS inlets was fully turbulent ($Re > 10\,000$). The inlets used in this study introduced a small delay ($\Delta t = 2.2$ s for DMS, $\Delta t = 1.2$ s for CO₂) between measured wind and atmospheric measurements, as well as minor loss of covariance at high frequencies (< 5 %). The methods used to estimate the delay and loss of flux are given in Bell et al. (2013).

Eddy covariance fluxes were computed for DMS and CO₂ as F_{DMS} or $F_{\text{CO}_2} = \sigma_{\text{air}}(w'c')$, where σ_{air} is the dry air density, w' is the fluctuation in vertical winds and c' is the delay-adjusted fluctuation in gas concentration. Average covariance fluxes were processed in 10 and 9.5 min intervals for DMS and CO₂, respectively (hereafter referred to as 10 min intervals). Momentum and sensible heat fluxes were also computed for 10 min intervals (see Bell et al., 2013).

Sampling intervals with a mean wind direction relative to the bow of > 90° were excluded from the final data set. CO₂ fluxes were also excluded from intervals when either (i) relative wind direction changed excessively ($SD > 10^\circ$), (ii) relative wind speed was low (< 1 m s⁻¹) or (iii) ΔCO_2 was low (< |30| ppm). DMS and CO₂ fluxes were quality controlled for excessive low-frequency flux as described in the Supplement of Bell et al. (2013). These quality control criteria excluded 62 % of the intervals for CO₂ and 55 % for DMS and significantly reduced the scatter in the data.

The Supplement related to this article is available online at <https://doi.org/10.5194/acp-17-9019-2017-supplement>.

Competing interests. The authors declare that they have no conflict of interest.

Acknowledgements. We thank the captain and crew of the R/V *Knorr* and the Woods Hole Marine Department for their assistance in carrying out this cruise. Funding for this research was provided by the NSF Atmospheric Chemistry Program (AGS-0851068, -0851472, -0851407 and -1134709) and the NSF Independent Research and Development Program. Adrian H. Callaghan acknowledges support from a Royal Society Shooter International Fellowship and from the National Science Foundation under grant OCE-1434866. Brian Ward acknowledges support from Science Foundation Ireland under grant 08/US/I1455 and from the FP7 Marie Curie Reintegration programme under grant 224776. We are grateful for constructive comments from our reviewers (Byron Blomquist, Ian Brooks and Bill Asher), which helped improve the paper. This study is a contribution to the international Surface Ocean Lower Atmosphere Study (SOLAS) programme.

Edited by: Jennifer G. Murphy

Reviewed by: Ian Brooks and William E. Asher

References

- Asher, W. E. and Wanninkhof, R.: The effect of bubble-mediated gas transfer on purposeful dual-gaseous tracer experiments, *J. Geophys. Res.-Oceans*, 103, 10555–10560, <https://doi.org/10.1029/98jc00245>, 1998.
- Asher, W. E., Karle, L. M., Higgins, B. J., Farley, P. J., Monahan, E. C., and Leifer, I. S.: The influence of bubble plumes on air-seawater gas transfer velocities, *J. Geophys. Res.-Oceans*, 101, 12027–12041, 1996.
- Asher, W. E., Edson, J., McGillis, W., Wanninkhof, R., Ho, D. T., and Litchendor, T.: Fractional area whitecap coverage and air-sea gas transfer velocities measured during GasEx-98, in: *Gas Transfer at Water Surfaces*, American Geophysical Union, 199–203, 2002.
- Bell, T. G., De Bruyn, W., Miller, S. D., Ward, B., Christensen, K. H., and Saltzman, E. S.: Air-sea dimethylsulfide (DMS) gas transfer in the North Atlantic: evidence for limited interfacial gas exchange at high wind speed, *Atmos. Chem. Phys.*, 13, 11073–11087, <https://doi.org/10.5194/acp-13-11073-2013>, 2013.
- Bell, T. G., De Bruyn, W., Marandino, C. A., Miller, S. D., Law, C. S., Smith, M. J., and Saltzman, E. S.: Dimethylsulfide gas transfer coefficients from algal blooms in the Southern Ocean, *Atmos. Chem. Phys.*, 15, 1783–1794, <https://doi.org/10.5194/acp-15-1783-2015>, 2015.
- Blomquist, B. W., Fairall, C. W., Huebert, B. J., Kieber, D. J., and Westby, G. R.: DMS sea-air transfer velocity: Direct measurements by eddy covariance and parameterization based on the NOAA/COARE gas transfer model, *Geophys. Res. Lett.*, 33, L07601, <https://doi.org/10.1029/2006gl025735>, 2006.
- Blomquist, B. W., Fairall, C. W., Huebert, B. J., and Wilson, S. T.: Direct measurement of the oceanic carbon monoxide flux by eddy correlation, *Atmos. Meas. Tech.*, 5, 3069–3075, <https://doi.org/10.5194/amt-5-3069-2012>, 2012.
- Blomquist, B. W., Huebert, B. J., Fairall, C. W., Bariteau, L., Edson, J. B., Hare, J. E., and McGillis, W. R.: Advances in air-sea CO₂ flux measurement by eddy correlation, *Bound.-Lay. Meteorol.*, 152, 245–276, <https://doi.org/10.1007/s10546-014-9926-2>, 2014.
- Callaghan, A. H. and White, M.: Automated processing of sea surface images for the determination of whitecap coverage, *J. Atmos. Ocean. Tech.*, 26, 383–394, <https://doi.org/10.1175/2008jtecho634.1>, 2009.
- Callaghan, A. H., de Leeuw, G., Cohen, L., and O’Dowd, C. D.: Relationship of oceanic whitecap coverage to wind speed and wind history, *Geophys. Res. Lett.*, 35, L23609, <https://doi.org/10.1029/2008gl036165>, 2008.
- Callaghan, A. H., Deane, G. B., and Stokes, M. D.: Two regimes of laboratory whitecap foam decay: Bubble-plume controlled and surfactant stabilized, *J. Phys. Oceanogr.*, 43, 1114–1126, <https://doi.org/10.1175/Jpo-D-12-0148.1>, 2013.
- Carpenter, L. J., Archer, S. D., and Beale, R.: Ocean-atmosphere trace gas exchange, *Chem. Soc. Rev.*, 41, 6473–6506, <https://doi.org/10.1039/c2cs35121h>, 2012.
- Cipriano, R. J. and Blanchard, D. C.: Bubble and aerosol spectra produced by a laboratory ‘breaking wave’, *J. Geophys. Res.-Oceans*, 86, 8085–8092, <https://doi.org/10.1029/JC086iC09p08085>, 1981.
- Dacey, J. W. H., Wakeham, S. G., and Howes, B. L.: Henry’s law constants for dimethylsulfide in fresh water and seawater, *Geophys. Res. Lett.*, 11, 991–994, 1984.
- Edson, J. B., DeGrandpre, M. D., Frew, N. M., and McGillis, W. R.: Investigations of air-sea gas exchange in the CoOP Coastal Air-Sea Chemical Exchange Project, *Oceanography*, 21, 34–45, <https://doi.org/10.5670/oceanog.2008.03>, 2008.
- Fairall, C. W., Bradley, E. F., Godfrey, J. S., Wick, G. A., Edson, J. B., and Young, G. S.: Cool-skin and warm-layer effects on sea surface temperature, *J. Geophys. Res.-Oceans*, 101, 1295–1308, <https://doi.org/10.1029/95jc03190>, 1996.
- Fairall, C. W., Hare, J. E., Edson, J. B., and McGillis, W.: Parameterization and micrometeorological measurement of air-sea gas transfer, *Bound.-Lay. Meteorol.*, 96, 63–105, 2000.
- Fairall, C. W., Yang, M., Bariteau, L., Edson, J. B., Helmig, D., McGillis, W., Pezoa, S., Hare, J. E., Huebert, B., and Blomquist, B.: Implementation of the Coupled Ocean-Atmosphere Response Experiment flux algorithm with CO₂, dimethyl sulfide, and O₃, *J. Geophys. Res.-Oceans*, 116, C00F09, <https://doi.org/10.1029/2010jc006884>, 2011.
- Goddijn-Murphy, L., Woolf, D. K., and Marandino, C.: Space-based retrievals of air-sea gas transfer velocities using altimeters: Calibration for dimethyl sulfide, *J. Geophys. Res.-Oceans*, 117, C08028, <https://doi.org/10.1029/2011jc007535>, 2012.
- Goddijn-Murphy, L., Woolf, D. K., Callaghan, A. H., Nightingale, P. D., and Shutler, J. D.: A reconciliation of empirical and mechanistic models of the air-sea gas transfer velocity, *J. Geophys. Res.-Oceans*, 121, 818–835, <https://doi.org/10.1002/2015jc011096>, 2016.

- Hoover, T. E. and Berkshire, D. C.: Effects of hydration on carbon dioxide exchange across an air–water interface, *J. Geophys. Res.*, 74, 456–464, 1969.
- Huebert, B. J., Blomquist, B. W., Hare, J. E., Fairall, C. W., Johnson, J. E., and Bates, T. S.: Measurement of the sea–air DMS flux and transfer velocity using eddy correlation, *Geophys. Res. Lett.*, 31, L23113, <https://doi.org/10.1029/2004gl021567>, 2004.
- Keeling, R. F.: On the role of large bubbles in air–sea gas exchange and supersaturation in the ocean, *J. Marine Res.*, 51, 237–271, <https://doi.org/10.1357/0022240933223800>, 1993.
- Kloster, S., Feichter, J., Maier-Reimer, E., Six, K. D., Stier, P., and Wetzell, P.: DMS cycle in the marine ocean–atmosphere system – a global model study, *Biogeosciences*, 3, 29–51, <https://doi.org/10.5194/bg-3-29-2006>, 2006.
- Landwehr, S., Miller, S. D., Smith, M. J., Saltzman, E. S., and Ward, B.: Analysis of the PKT correction for direct CO₂ flux measurements over the ocean, *Atmos. Chem. Phys.*, 14, 3361–3372, <https://doi.org/10.5194/acp-14-3361-2014>, 2014.
- Landwehr, S., O’Sullivan, N., and Ward, B.: Direct flux measurements from mobile platforms at sea: Motion and airflow distortion corrections revisited, *J. Atmos. Ocean. Tech.*, 32, 1163–1178, <https://doi.org/10.1175/jtech-d-14-00137.1>, 2015.
- Le Quéré, C., Moriarty, R., Andrew, R. M., Peters, G. P., Ciais, P., Friedlingstein, P., Jones, S. D., Sitch, S., Tans, P., Arneeth, A., Boden, T. A., Bopp, L., Bozec, Y., Canadell, J. G., Chini, L. P., Chevallier, F., Cosca, C. E., Harris, I., Hoppema, M., Houghton, R. A., House, J. I., Jain, A. K., Johannessen, T., Kato, E., Keeling, R. F., Kitidis, V., Klein Goldewijk, K., Koven, C., Landa, C. S., Landschützer, P., Lenton, A., Lima, I. D., Marland, G., Mathis, J. T., Metzl, N., Nojiri, Y., Olsen, A., Ono, T., Peng, S., Peters, W., Pfeil, B., Poulter, B., Raupach, M. R., Regnier, P., Rödenbeck, C., Saito, S., Salisbury, J. E., Schuster, U., Schwinger, J., Séférian, R., Segschneider, J., Steinhoff, T., Stocker, B. D., Sutton, A. J., Takahashi, T., Tilbrook, B., van der Werf, G. R., Viovy, N., Wang, Y.-P., Wanninkhof, R., Wiltshire, A., and Zeng, N.: Global carbon budget 2014, *Earth Syst. Sci. Data*, 7, 47–85, <https://doi.org/10.5194/essd-7-47-2015>, 2015.
- Liss, P. S. and Merlivat, L.: Air–sea gas exchange rates: introduction and synthesis, in: *The role of air–sea exchange in geochemical cycling*, edited by: Buatmenard, P., Reidel, 113–127, 1986.
- Liss, P. S. and Slater, P. G.: Flux of gases across the air–sea interface, *Nature*, 247, 181–184, 1974.
- Marandino, C. A., de Bruyn, W. J., Miller, S. D., and Saltzman, E. S.: Eddy correlation measurements of the air/sea flux of dimethylsulfide over the North Pacific Ocean, *J. Geophys. Res.-Atmos.*, 112, D03301, <https://doi.org/10.1029/2006jd007293>, 2007.
- McGillis, W. R., Dacey, J. W. H., Frew, N. M., Bock, E. J., and Nelson, R. K.: Water–air flux of dimethylsulfide, *J. Geophys. Res.-Oceans*, 105, 1187–1193, 2000.
- McGillis, W. R., Edson, J. B., Hare, J. E., and Fairall, C. W.: Direct covariance air–sea CO₂ fluxes, *J. Geophys. Res.-Oceans*, 106, 16729–16745, 2001.
- Melville, W. K. and Matusov, P.: Distribution of breaking waves at the ocean surface, *Nature*, 417, 58–63, 2002.
- Miller, S. D., Hristov, T. S., Edson, J. B., and Friehe, C. A.: Platform motion effects on measurements of turbulence and air–sea exchange over the open ocean, *J. Atmos. Ocean. Tech.*, 25, 1683–1694, <https://doi.org/10.1175/2008jtecho547.1>, 2008.
- Miller, S. D., Marandino, C., de Bruyn, W., and Saltzman, E. S.: Air–sea gas exchange of CO₂ and DMS in the North Atlantic by eddy covariance, *Geophys. Res. Lett.*, 36, L15816, <https://doi.org/10.1029/2009gl038907>, 2009.
- Miller, S. D., Marandino, C., and Saltzman, E. S.: Ship-based measurement of air–sea CO₂ exchange by eddy covariance, *J. Geophys. Res.-Atmos.*, 115, D02304, <https://doi.org/10.1029/2009jd012193>, 2010.
- Pereira, R., Schneider-Zapp, K., and Upstill-Goddard, R. C.: Surfactant control of gas transfer velocity along an offshore coastal transect: results from a laboratory gas exchange tank, *Biogeosciences*, 13, 3981–3989, <https://doi.org/10.5194/bg-13-3981-2016>, 2016.
- Rhee, T. S., Nightingale, P. D., Woolf, D. K., Caulliez, G., Bowyer, P., and Andreae, M. O.: Influence of energetic wind and waves on gas transfer in a large wind-wave tunnel facility, *J. Geophys. Res.-Oceans*, 112, C05027, <https://doi.org/10.1029/2005jc003358>, 2007.
- Saltzman, E. S., King, D. B., Holmen, K., and Leck, C.: Experimental determination of the diffusion coefficient of dimethylsulfide in water, *J. Geophys. Res.-Oceans*, 98, 16481–16486, 1993.
- Saltzman, E. S., De Bruyn, W. J., Lawler, M. J., Marandino, C. A., and McCormick, C. A.: A chemical ionization mass spectrometer for continuous underway shipboard analysis of dimethylsulfide in near-surface seawater, *Ocean Sci.*, 5, 537–546, <https://doi.org/10.5194/os-5-537-2009>, 2009.
- Scanlon, B. and Ward, B.: Oceanic wave breaking coverage separation techniques for active and maturing whitecaps, *Methods in Oceanography*, 8, 1–12, <https://doi.org/10.1016/j.mio.2014.03.001>, 2013.
- Schwendeman, M. and Thomson, J.: Observations of whitecap coverage and the relation to wind stress, wave slope, and turbulent dissipation, *J. Geophys. Res.-Oceans*, 120, 8346–8363, <https://doi.org/10.1002/2015jc011196>, 2015.
- Stefels, J., Steinke, M., Turner, S., Malin, G., and Belviso, S.: Environmental constraints on the production and removal of the climatically active gas dimethylsulphide (DMS) and implications for ecosystem modelling, *Biogeochemistry*, 83, 245–275, <https://doi.org/10.1007/s10533-007-9091-5>, 2007.
- Virkkula, A., Teinilä, K., Hillamo, R., Kerminen, V.-M., Saarikoski, S., Aurela, M., Koponen, I. K., and Kulmala, M.: Chemical size distributions of boundary layer aerosol over the Atlantic Ocean and at an Antarctic site, *J. Geophys. Res.-Atmos.*, 111, D05306, <https://doi.org/10.1029/2004jd004958>, 2006.
- Wanninkhof, R.: Relationship between wind speed and gas exchange over the ocean, *J. Geophys. Res.-Oceans*, 97, 7373–7382, 1992.
- Wanninkhof, R. and Knox, M.: Chemical enhancement of CO₂ exchange in natural waters, *Limnol. Oceanogr.*, 41, 689–697, <https://doi.org/10.4319/lo.1996.41.4.0689>, 1996.
- Wanninkhof, R., Ledwell, J. R., and Broecker, W. S.: Gas exchange–wind speed relation measured with sulfur hexafluoride on a lake, *Science*, 227, 1224–1226, <https://doi.org/10.1126/science.227.4691.1224>, 1985.
- Watson, A. J., Upstill-Goddard, R. C., and Liss, P. S.: Air–sea gas exchange in rough and stormy seas measured by a dual-tracer technique, *Nature*, 349, 145–147, 1991.

- Weiss, R. F.: Carbon dioxide in water and seawater: The solubility of a non-ideal gas, *Mar. Chem.*, 2, 203–215, [https://doi.org/10.1016/0304-4203\(74\)90015-2](https://doi.org/10.1016/0304-4203(74)90015-2), 1974.
- Woolf, D. K.: Bubbles and the air-sea transfer velocity of gases, *Atmos. Ocean*, 31, 517–540, 1993.
- Woolf, D. K.: Bubbles and their role in gas exchange, in: *The Sea Surface and Global Change*, edited by: Liss, P. S. and Duce, R. A., Cambridge University Press, Cambridge, 173–205, 1997.
- Woolf, D. K.: Parametrization of gas transfer velocities and sea-state-dependent wave breaking, *Tellus B*, 57, 87–94, 2005.
- Woolf, D. K., Leifer, I. S., Nightingale, P. D., Rhee, T. S., Bowyer, P., Caulliez, G., de Leeuw, G., Larsen, S. E., Liddicoat, M., Baker, J., and Andreae, M. O.: Modelling of bubble-mediated gas transfer: Fundamental principles and a laboratory test, *J. Marine Syst.*, 66, 71–91, <https://doi.org/10.1016/j.jmarsys.2006.02.011>, 2007.
- Woolf, D. K., Land, P. E., Shutler, J. D., Goddijn-Murphy, L. M., and Donlon, C. J.: On the calculation of air-sea fluxes of CO₂ in the presence of temperature and salinity gradients, *J. Geophys. Res.-Oceans*, 121, 1229–1248, <https://doi.org/10.1002/2015jc011427>, 2016.
- Yang, M., Blomquist, B. W., Fairall, C. W., Archer, S. D., and Huebert, B. J.: Air-sea exchange of dimethylsulfide in the Southern Ocean: Measurements from SO GasEx compared to temperate and tropical regions, *J. Geophys. Res.-Oceans*, 116, C00F05, <https://doi.org/10.1029/2010jc006526>, 2011.
- Yang, M., Beale, R., Liss, P., Johnson, M., Blomquist, B., and Nightingale, P.: Air-sea fluxes of oxygenated volatile organic compounds across the Atlantic Ocean, *Atmos. Chem. Phys.*, 14, 7499–7517, <https://doi.org/10.5194/acp-14-7499-2014>, 2014.